

# Shifts in the Properties of the Higgs Boson from Radion Mixing \*

**J.L. Hewett and T.G. Rizzo**

Stanford Linear Accelerator Center  
Stanford University  
Stanford CA 94309, USA

## Abstract

We examine how mixing between the Standard Model Higgs boson,  $h$ , and the radion present in the Randall-Sundrum model of localized gravity modifies the expected properties of the Higgs boson. In particular, we demonstrate that the total and partial decay widths of the Higgs, as well as the  $h \rightarrow gg$  branching fraction, can be substantially altered from their Standard Model expectations. The remaining branching fractions are modified less than  $\lesssim 5\%$  for most of the parameter space volume.

---

\*Work supported by the Department of Energy, Contract DE-AC03-76SF00515

The Randall-Sundrum (RS) model of localized gravity [1] offers a potential solution to the hierarchy problem that can be tested at present and future accelerators [2]. In the original version of this model, the Standard Model (SM) fields are confined to one of two branes that are embedded in a 5-dimensional anti-de Sitter space ( $\text{AdS}_5$ ) described by the metric  $ds^2 = e^{-2k|y|}\eta_{\mu\nu}dx^\mu dx^\nu - dy^2$ , with  $y = r_c\phi$  where  $r_c$  is the compactification radius and  $\phi$  describes the 5<sup>th</sup> dimension. The parameter  $k$  characterizes the curvature of the 5-dimensional space and is naturally of order the Planck scale. The two branes form the boundaries of the  $\text{AdS}_5$  slice and gravity is localized on the brane located at  $y = 0$ . Mass parameters on the Standard Model brane, located at  $y = r_c\pi$ , are red-shifted compared to those on the  $y = 0$  brane and are given by  $\Lambda_\pi = \overline{M}_{Pl}e^{-kr_c\pi}$ , where  $\overline{M}_{Pl}$  is the reduced Planck scale. In order to address the hierarchy problem,  $\Lambda_\pi \sim \text{TeV}$  and hence the separation between the two branes,  $r_c$ , must have a value of  $kr_c \sim 11 - 12$ . A number of authors [3] have demonstrated that this quantity can be naturally stabilized by a mechanism which leads directly to the existence of a massive bulk scalar field.

Fluctuations about the stabilized RS configuration allow for two massless excitations described in the metric by  $\eta_{\mu\nu} \rightarrow g_{\mu\nu}(x)$  and  $r_c \rightarrow T(x)$ . The first corresponds to the graviton and  $T(x)$  is a new scalar field arising from the  $g_{55}$  component of the metric and is known as the radion ( $r_0$ ). This scalar field corresponds to a quantum excitation of the separation between the two branes. The mass of the radion is proportional to the backreaction of the bulk scalar vacuum expectation value (vev) on the metric. Generally, one expects that the radion mass should be in the range of a few  $\times 10 \text{ GeV} \leq m_{r_0} \leq \Lambda_\pi$ , where the lower limit arises from radiative corrections and the upper bound is the cutoff of the effective field theory. The radion mass  $m_{r_0}$  is then expected to be below the scale  $\Lambda_\pi$  implying that the radion may be the lightest new field present in the RS model. The radion couples to fields on the Standard Model brane via the trace of the stress-energy tensor with a strength  $\Lambda \propto \Lambda_\pi$

of order the TeV scale,

$$\mathcal{L}_{eff} = -r_0(x) T_\mu^\mu / \Lambda. \quad (1)$$

Note that  $\Lambda = \sqrt{3}\Lambda_\pi$  in the notation of Ref. [2]. This leads to gauge and matter couplings for the radion that are qualitatively similar to those of the SM Higgs boson. The collider production and decay of the RS radion has been examined by a number of authors [4, 5] and has been recently reviewed by Kribs [6].

On general grounds of covariance, the radion may mix with the SM Higgs field, which is constrained to the TeV brane, through an interaction term of the form

$$S_{rH} = -\xi \int d^4x \sqrt{-g_{ind}} R^{(4)}[g_{ind}] H^\dagger H. \quad (2)$$

Here  $H$  is the Higgs doublet field,  $R^{(4)}[g_{ind}]$  is the 4-d Ricci scalar constructed out of the induced metric  $g_{ind}$  on the SM brane, and  $\xi$  is a dimensionless mixing parameter assumed to be of order unity and with unknown sign. The above action induces kinetic mixing between the  $r_0$  and  $h_0$  fields. The resulting Lagrangian can be diagonalized by a set of field redefinitions and rotations [7],

$$\begin{aligned} h_0 &= Ah + Br, \\ r_0 &= Ch + Dr, \end{aligned} \quad (3)$$

with

$$\begin{aligned} A &= \cos\theta - 6\xi\gamma/Z \sin\theta, \\ B &= \sin\theta + 6\xi\gamma/Z \cos\theta, \\ C &= -\sin\theta/Z, \\ D &= \cos\theta/Z, \end{aligned} \quad (4)$$

where  $h, r$  represent the physical fields, and

$$\gamma = \frac{v}{\Lambda}, \quad (5)$$

$$Z^2 = 1 + 6\xi(1 - 6\xi)\gamma^2,$$

with  $v \simeq 246$  GeV being the SM vacuum expectation value. The factor  $Z$  serves to bring the physical radion kinetic term to canonical form and as such it must satisfy  $Z > 0$ . For a fixed value of  $\gamma$  this implies that the range of  $\xi$  is bounded, *i.e.*,  $\xi_- \leq \xi \leq \xi_+$ , where

$$\xi_{\pm} = \frac{1}{12}[1 \pm (1 + 4/\gamma^2)^{1/2}], \quad (6)$$

For example, if  $\gamma$  takes on the natural values  $\gamma = 0.2(0.1)$  then  $\xi$  must lie in the approximate range  $-0.754 \leq \xi \leq 0.921$  ( $-1.585 \leq \xi \leq 1.752$ ). The masses of the physical states,  $r, h$ , are then given by

$$m_{\pm}^2 = \frac{1}{2}[T \pm \sqrt{T^2 - 4F}], \quad (7)$$

where  $m_+(m_-)$  is the larger(smaller) of the two masses and

$$T = (1 + t^2)m_{h_0}^2 + m_{r_0}^2/Z, \quad (8)$$

$$F = m_{h_0}^2 m_{r_0}^2 / Z^2,$$

with  $m_{h_0, r_0}$  being the weak interaction eigenstate masses and  $t = 6\xi\gamma/Z$ . This mixing will clearly affect the phenomenology of both the radion and Higgs fields. In particular, the bounds on the Higgs mass from the standard global fit to precision electroweak data are modified, allowing for a Higgs boson (and radion) mass of order several hundred GeV [7]. Here, we examine the modifications to the properties of the Higgs boson, in particular its decay widths and branching fractions, induced by this mixing and find that substantial differences from the SM expectations can be obtained.

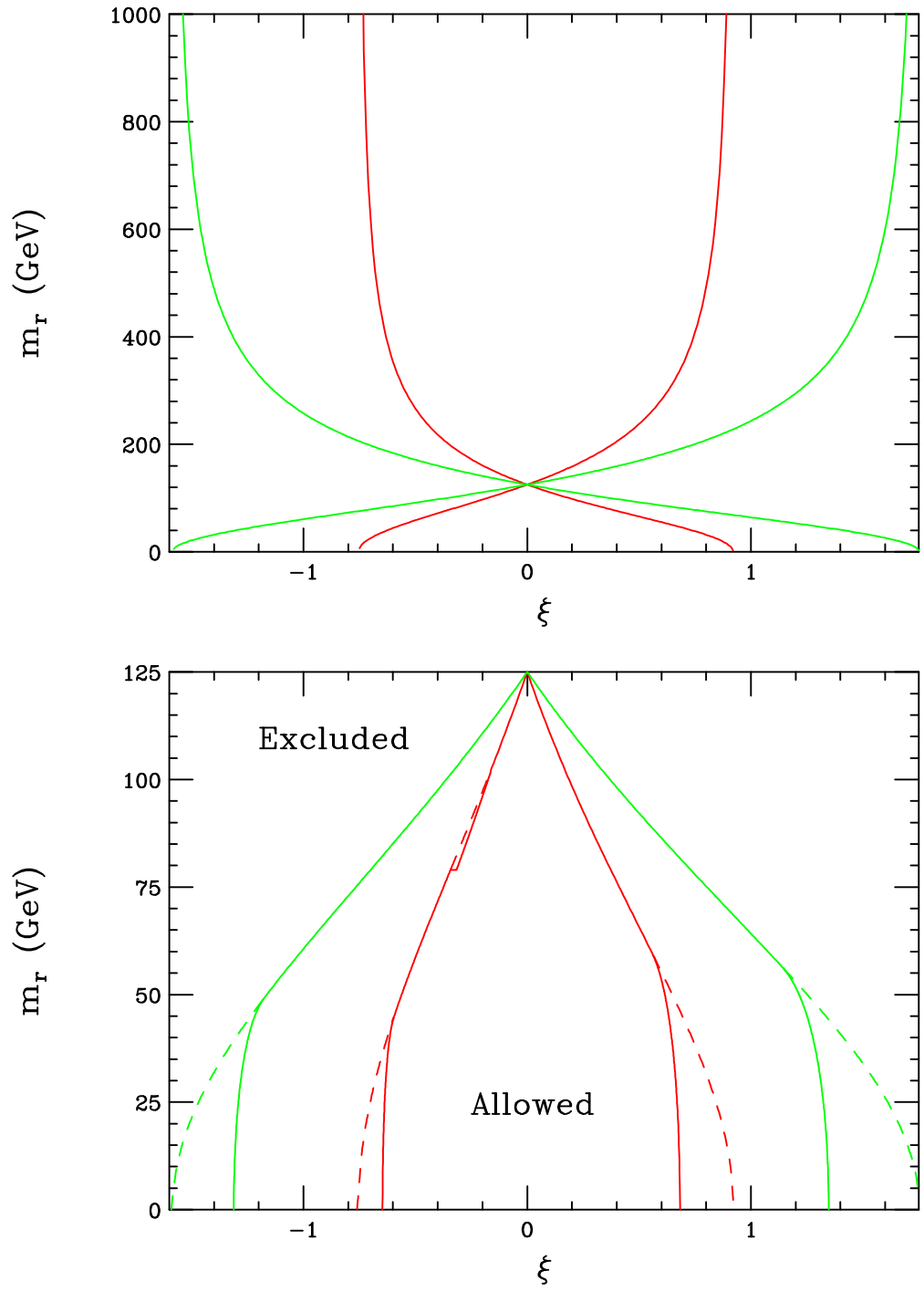


Figure 1: Constraints on the mass of the radion assuming  $m_h = 125$  GeV as a function of  $\xi$  as described in the text for  $\gamma = 0.1$ (green, outer curves) and  $0.2$ (red, inner curves). The allowed region lies between the solid curves. In the lower panel the regions excluded by LEP searches are also shown and they lie between the corresponding solid and dashed curves.

To make predictions in this scenario we need to specify four parameters: the masses of the physical Higgs and radion fields,  $m_{h,r}$ , the mixing parameter  $\xi$ , and the ratio  $\gamma = v/\Lambda$ . Clearly this ratio cannot be too large as  $\Lambda_\pi$  is already bounded from below by collider and electroweak precision data [2]; Tevatron data for contact interactions yields the constraints  $\Lambda_\pi \gtrsim 300, 1500, 4500$  GeV for  $k/\overline{M}_{Pl} = 1.0, 0.1, 0.01$ , respectively. Curvature constraints suggest that  $k/\overline{M}_{Pl} \leq 0.1$  [2], which in turn implies  $v/\Lambda \lesssim 0.1$ . For definiteness we will relax this bound somewhat and take  $v/\Lambda \leq 0.2$  along with a physical Higgs mass of 125 GeV in our analysis. We note that large absolute values of  $\xi$  and wide ranges of  $v/\Lambda$  have been entertained in the literature.

The values of the two physical masses themselves are not arbitrary. When we require the weak eigenstate mass-squared parameters of the unmixed radion and Higgs fields to be real, as is demanded by hermiticity, we obtain an additional constraint on the ratio of the physical radion and Higgs masses which depends on both  $\xi$  and  $\gamma$ . Defining the ratio  $r = (m_+/m_-)^2$ , one finds that these two conditions require that  $r$  must be bounded from below by

$$r_{min} = 1 + 2t^2 \pm 2|t|\sqrt{1+t^2}, \quad (9)$$

where the sign depends on the ordering of  $m_h$  and  $m_r$ . Note that this bound implies that it is disfavored for the radion to have a mass near that of the Higgs when there is significant mixing. The resulting excluded region is shown in Fig. 1 for the demonstrative case of  $m_h = 125$  GeV. These constraints are found to be somewhat restrictive. The low mass region for the radion is also partially excluded by direct searches at LEP as can be seen from the figure. In calculating the LEP constraints, we fixed  $v/\Lambda$  to the conservative values of  $v/\Lambda = 0.2(0.1)$  while varying  $\xi$ , and converted the LEP Higgs search bounds [8] into constraints for the radion using the appropriate set of rescaling factors. While some of the low mass region for the radion is eliminated for these values of the parameters, the parameter

space for a light radion is certainly not closed. As one decreases the assumed fixed value of  $v/\Lambda$ , the size of the allowed low mass region grows since the radion couplings to the  $Z$  boson are rapidly shrinking.

Once  $\xi, \gamma$  and  $m_{h,r}$  are specified, the angle  $\theta$  describing the rotations into the Higgs-radion physical states becomes calculable; one finds that

$$\begin{aligned}\tan 2\theta &= \frac{2tZ^2m_{h_0}^2}{m_{r_0}^2 - m_{h_0}^2(Z^2 - 36\xi^2\gamma^2)}, \\ \sin 2\theta &= \frac{2tm_{h_0}^2}{m_r^2 - m_h^2}.\end{aligned}\tag{10}$$

The weak basis masses are given by

$$m_{h_0}^2 = \frac{m_+^2 + m_-^2 \pm \sqrt{(m_+^2 + m_-^2)^2 - (2m_+m_-)^2(1+t^2)}}{2(1+t^2)},\tag{11}$$

with the sign chosen positive(negative) when  $m_h(m_r)$  is identified with  $m_\pm$ . In either case one obtains  $m_{r_0} = Zm_+m_-/m_{h_0}$ .

We now turn our attention to the properties of the Higgs boson in this model when mixing with the radion is included. Following the notation of Csaki *et al.* [7], the couplings of the physical Higgs to the SM fermions and massive gauge bosons  $V = W, Z$  is now given by

$$\mathcal{L} = \frac{-1}{v}(m_f\bar{f}f - m_V^2V_\mu V^\mu)[\cos\theta - t\sin\theta - \frac{v}{\Lambda}\sin\theta/Z]h,\tag{12}$$

where the angle  $\theta$  is defined above and can now be calculated in terms of the four parameters  $\xi, v/\Lambda$ , and the physical Higgs and radion masses. Note that the shifts to the fermionic and massive gauge boson couplings are identical. Denoting the combinations  $\alpha = \cos\theta - t\sin\theta$

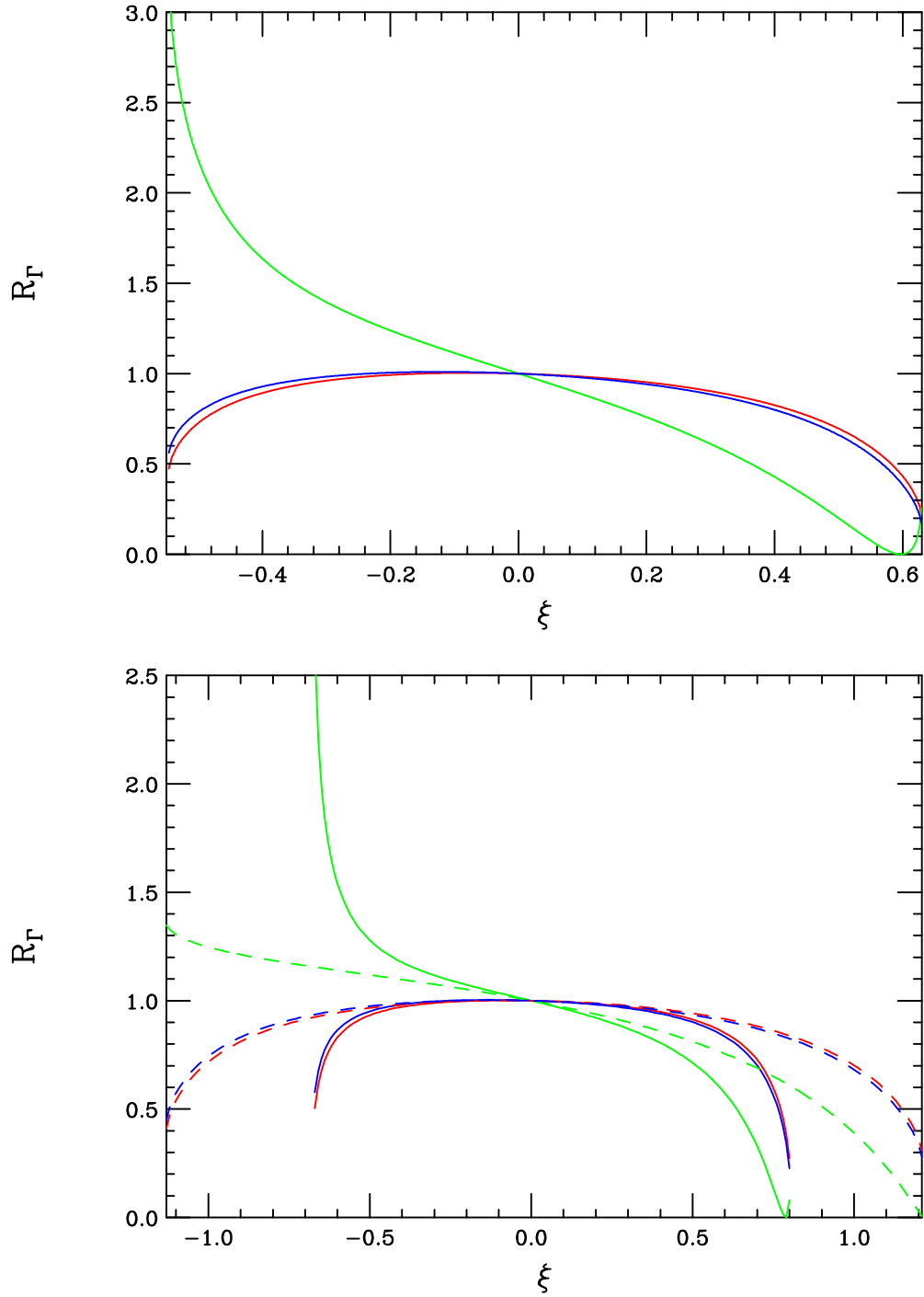


Figure 2: Ratio of Higgs partial widths to their SM values,  $R_\Gamma$ , as a function of  $\xi$  assuming a physical Higgs mass of 125 GeV: red for fermion pairs or massive gauge boson pairs, green for gluons and blue for photons. This corresponds to gluons, photons,  $V\bar{V}$  from bottom to top on the right. In the top panel we assume  $m_r = 300$  GeV and  $v/\Lambda = 0.2$ . In the bottom panel the solid(dashed) curves are for  $m_r = 500(300)$  GeV and  $v/\Lambda = 0.2(0.1)$ .



and  $\beta = -\sin\theta/Z$ , the corresponding Higgs coupling to gluons can be written as

$$\mathcal{L} = c_g \frac{\alpha_s}{8\pi} G_{\mu\nu} G^{\mu\nu} h, \quad (13)$$

with

$$c_g = \frac{-1}{2v} \left[ \left( \alpha + \frac{v}{\Lambda} \beta \right) F_g - 2b_3 \beta \frac{v}{\Lambda} \right]. \quad (14)$$

Here, the first term is the usual one-loop top-quark contribution to the  $ggh$  coupling, whereas the second term arises from the trace anomaly and appears solely from the mixing.  $b_3 = 7$  is the  $SU(3)$   $\beta$ -function and  $F_g$  is a well-known kinematic function of the ratio of masses of the top-quark to the physical Higgs boson [9]. Similarly the physical Higgs coupling to two photons is now given by

$$\mathcal{L} = c_\gamma \frac{\alpha_{em}}{8\pi} F_{\mu\nu} F^{\mu\nu} h, \quad (15)$$

where

$$c_\gamma = \frac{1}{v} \left[ -\left( \alpha + \frac{v}{\Lambda} \beta \right) F_\gamma + (b_2 + b_Y) \beta \frac{v}{\Lambda} \right]. \quad (16)$$

Here,  $b_2 = 19/6$  and  $b_Y = -41/6$  are the  $SU(2) \times U(1)$   $\beta$ -functions and  $F_\gamma$  is another well-known kinematic function [9] of the ratios of the  $W$  boson and top-quark masses to the physical Higgs mass, and second term again originates from the trace anomaly. Note that in the simultaneous limits  $\alpha \rightarrow 1$ ,  $\beta \rightarrow 0$  we recover the usual SM results. From these expressions we can now compute the modifications to the various decay widths and branching fractions of the SM Higgs due to mixing with the radion.

Fig. 2 shows the ratio of the various Higgs partial widths in comparison to their SM expectations as a function of the parameter  $\xi$  for sample values of  $m_r$  and  $\frac{v}{\Lambda}$  and assuming that  $m_h = 125$  GeV. The range of the curves reflects the allowed parameter region for  $\xi$ . Several features are immediately apparent: (i) the shifts in the widths to  $\bar{f}f/VV$  and  $\gamma\gamma$

final states are very similar; this is due to the relatively large magnitude of  $F_\gamma$  while the combination  $b_2 + b_Y$  is rather small. (ii) On the otherhand, the shift for the  $gg$  final state can be substantial; here,  $F_g$  is numerically smaller than  $F_\gamma$  and  $b_3$  is quite large, resulting in a large contribution from the trace anomaly term. (iii) For relatively light radions with a lower value of  $\Lambda$ , the Higgs decay width into the  $gg$  final state can be vanishingly small. This is due to a strong destructive interference between the two contributions to the amplitude for values of  $\xi$  near  $-1$ . (iv) Increasing the value of  $m_r$  has less of an effect than does a decrease in the ratio  $\frac{v}{\Lambda}$ .

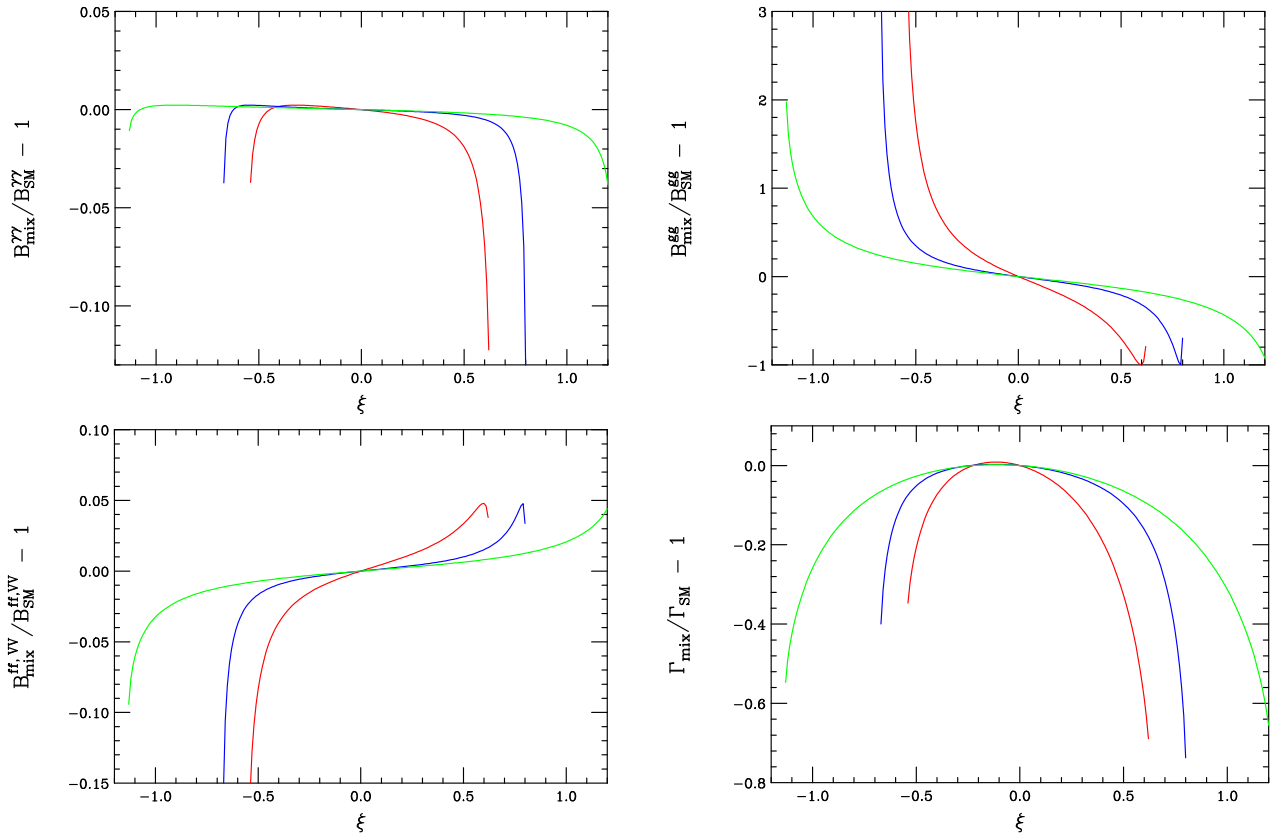


Figure 3: The ratio of the Higgs branching fraction into  $\gamma\gamma$ ,  $gg$ ,  $f\bar{f}$ , and  $VV$  final states as labeled, as well as for the total width, with radion mixing to that of the SM as a function of  $\xi$ . The red (blue; green) curves represent the choice  $m_r = 300$  GeV,  $v/\Lambda = 0.2$  (500, 0.2; 300, 0.1), and correspond to the curves which have the most limited (central; largest) range of  $\xi$ , respectively, in the figure.

The deviation from SM expectations for the various branching fractions, as well as the total width, of the Higgs are displayed in Fig. 3 as a function of the mixing parameter  $\xi$ . As above, the range of the curves reflects the allowed parameter region for  $\xi$ . We see that the gluon branching fraction and the total width may be drastically different than that of the SM. As we will see below, the former may greatly affect the Higgs production cross section at the LHC. However, the  $\gamma\gamma$ ,  $f\bar{f}$ , and  $VV$  (where  $V = W, Z$ ) branching fractions only receive small corrections to their SM values, of order  $\lesssim 5 - 10\%$  for almost all of the parameter region except near the edges of the parameter space. Observation of these shifts will require the precise determination of the Higgs branching fractions which is obtainable at a future high energy  $e^+e^-$  Linear Collider [10]. Once these measurements are performed, constraints on the radion parameter space may be extracted as will be discussed below. These small changes in the  $ZZh$  and  $hb\bar{b}$  couplings of the Higgs boson can also lead to small reductions in the Higgs search reach from LEP II. This is presented in Fig. 4 for several sets of parameters; except for extreme parameter cases this reduction in reach is rather modest.

At the LHC, the dominant production mechanism and signal for a light Higgs boson is gluon-gluon fusion through a triangle graph with subsequent decay into  $\gamma\gamma$ . Both the production cross section and the  $\gamma\gamma$  branching fraction are modified by mixing with the radion, leading to the results illustrated in Fig. 5. This figure shows that the Higgs production rate in this channel at the LHC can be either significantly reduced or somewhat enhanced in comparison to the expectations of the SM due to the effects of mixing. For some values of the parameters the reduction can be by more than an order of magnitude which could seriously hinder the discovery of the Higgs via this channel at the LHC.

The s-channel production of the Higgs boson at a high energy photon photon collider is an important channel for determining the properties of the Higgs. In Fig. 6 we see that decreases in the production rate of the Higgs compared to SM expectations can also occur

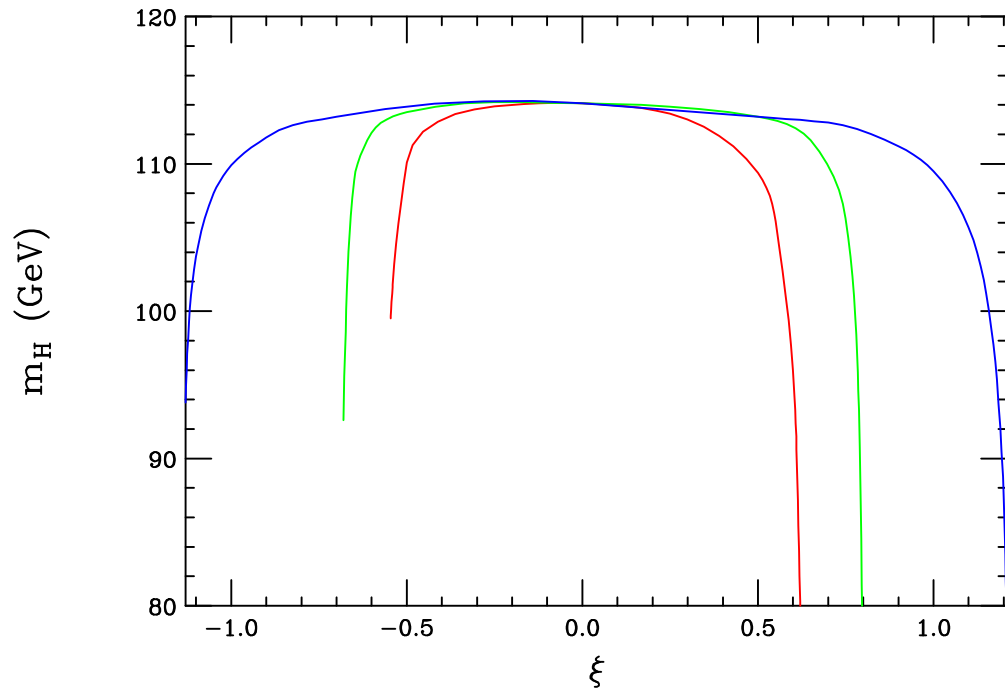


Figure 4: Lower bound on the mass of the Higgs boson from direct searches at LEP as a function of  $\xi$  including the effects of mixing. The red (green; blue) curves correspond to the choice  $m_r = 300$  GeV,  $v/\Lambda = 0.2$  (300, 0.1; 500, 0.2) and represent the curves from bottom to top.

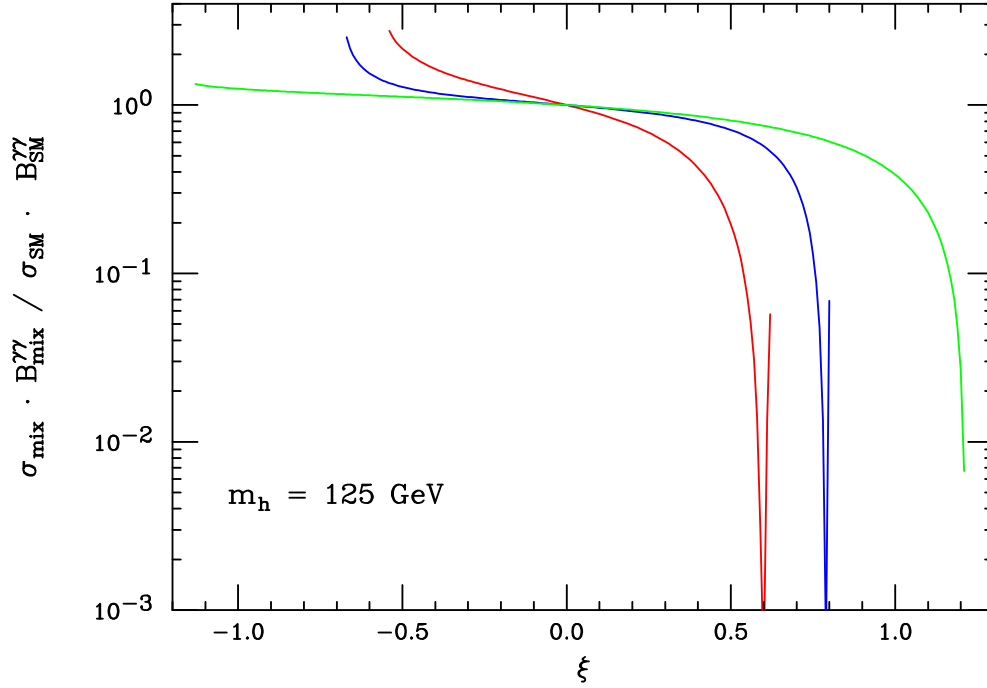


Figure 5: The ratio of production cross section times branching fraction for  $pp \rightarrow h \rightarrow \gamma\gamma$  via gluon fusion with radion mixing to the SM expectations as a function of  $\xi$ . The Higgs mass is taken to be 125 GeV. The red (blue; green) curves correspond to the choice  $m_r = 300$  GeV,  $v/\Lambda = 0.2$  (500, 0.2; 300, 0.1), from left to right on the RHS of the figure.

in the reaction  $\gamma\gamma \rightarrow h \rightarrow b\bar{b}$  when mixing with the radion is included. Again, once such mixing is taken into account, the event rate is reduced, possibly hampering the statistical ability of a future high energy photon collider to measure the Higgs properties. However, note that the potential reductions in rate for this channel are not as drastic as those which may be realized at the LHC.

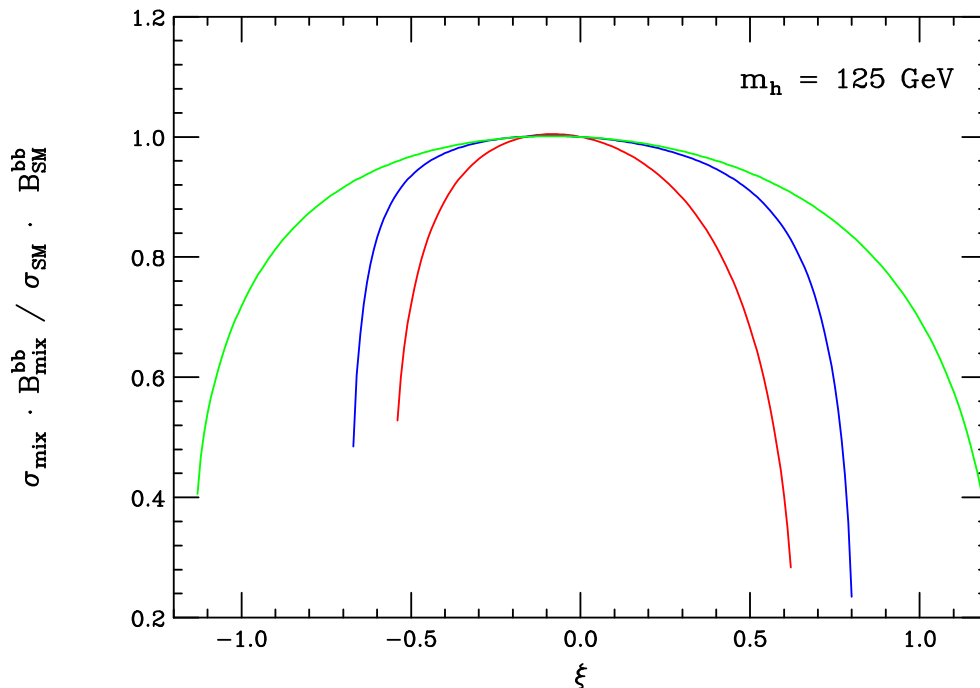


Figure 6: The ratio of production cross section times branching fraction for  $\gamma\gamma \rightarrow h \rightarrow b\bar{b}$  with radion mixing to the SM expectations as a function of  $\xi$ . The Higgs mass is taken to be 125 GeV. The red (blue; green) curves, corresponding to the bottom (middle, top) curves, represent the parameter choices  $m_r = 300$  GeV,  $v/\Lambda = 0.2$  (500, 0.2; 300, 0.1).

Once data from both the LHC and the Linear Collider (LC) is available, the radion parameter space can be explored using both direct searches and indirect measurements. In fact, the precision measurements of the Higgs boson couplings discussed above can be used to constrain the radion parameter space beyond what may be possible via direct searches for the radion. For purposes of demonstration, let us assume that the LHC and LC determine, within their capabilities, that the Higgs couplings are consistent with the predictions of the SM. Using the expectations for Higgs production at the LHC and LC from the analyses

contained in Ref. [10], we derive the resulting excluded regions in the  $\xi - m_r$  parameter plane. This is displayed in Fig. 7 for various values of  $v/\Lambda$  for the sample case of  $m_h = 125$  GeV. In this figure, the allowed region lies between the corresponding pair of vertical curves. Here, we see that if such a set of measurements of the Higgs properties are realized, then a large fraction of the radion parameter space would be excluded. Direct radion searches at these colliders would fully cover the lower portion of the remaining parameter space up to the radion search reach. Together, the direct and indirect constraints would then only allow for a high mass radion with small mixing as a possibility under this scenario.

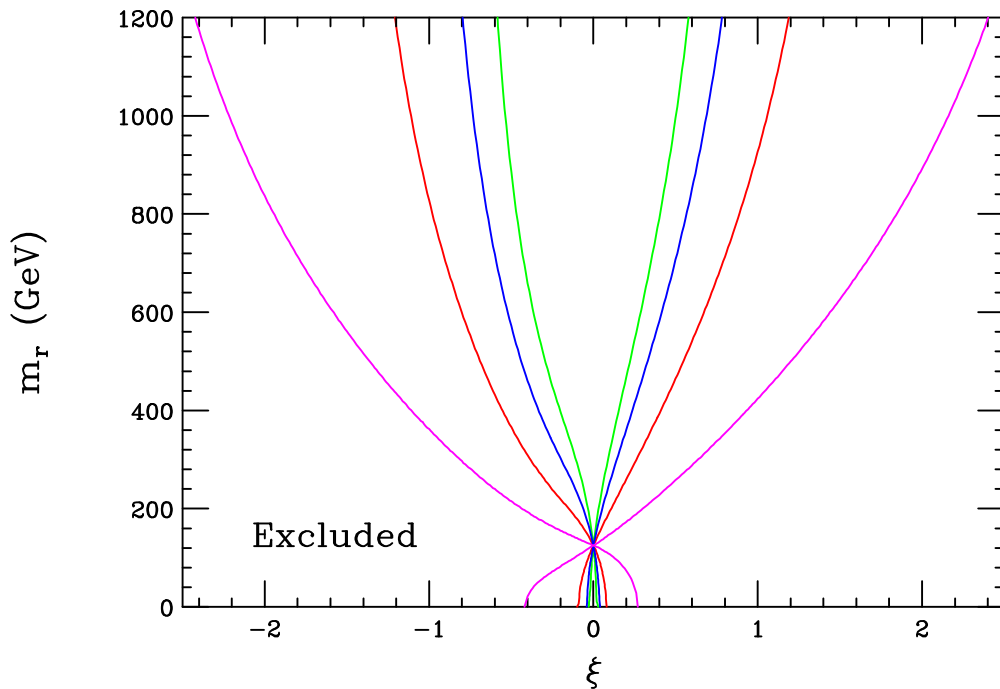


Figure 7: 95% CL indirect bounds on the mass and mixing of the radion arising from the precision measurements of the Higgs couplings obtainable at the LHC and a Linear Collider for a Higgs mass of 125 GeV. The allowed region lies between the corresponding pair of vertical curves. From the inner to outer curves, they represent the parameter values  $v/\Lambda = 0.2, 0.15, 0.10,$  and  $0.05,$  respectively.

Lastly, we note that the patterns of the shifts in the Higgs boson properties due to radion mixing are distinct from those in other models of new physics. For example, consider the two Higgs double model [9]. In this model, the ratio of the  $hVV$  coupling to its SM

value is given by  $\sin(\beta - \alpha)$  and the similar ratio for the  $ht\bar{t}$  coupling is  $\cos\alpha/\sin\beta$ , where  $\tan\beta$  is the ratio of vevs of the two Higgs doublets and  $\alpha$  is the mixing angle between the two doublets. In one variant of this model, the corresponding ratio of the  $hb\bar{b}$  coupling is equal, up to a sign, of that for the  $ht\bar{t}$  coupling, while in a second version of the model the  $hb\bar{b}$  ratio is  $-\sin\alpha/\cos\beta$ . In either case, this spectrum of couplings cannot be reproduced via radion mixing.

In summary, we see that Higgs-radion mixing, which is present in some extra dimensional scenarios, can have a substantial effect on the properties of the Higgs boson. These modifications affect the total and partial widths, as well as the branching fractions, of Higgs decay into various final states. This, in turn, can significantly alter the expectations for Higgs production at LEP, the LHC, and a photon collider. For some regions of the parameters, the size of these shifts in the Higgs widths and branching fractions may require the precision of a Linear Collider in order to be studied in detail.

Note Added: A related paper [11] appeared on the arXiv four months after this work and one year after a preliminary version of this work was presented at summer conferences [12].

## References

- [1] L. Randall and R. Sundrum, Phys. Rev. Lett. **83**, 3370 (1999); Phys. Rev. Lett. **83**, 4690 (1999).
- [2] For an overview of RS phenomenology, see H. Davoudiasl, J.L. Hewett and T.G. Rizzo, Phys. Rev. Lett. **84**, 2080 (2000); Phys. Lett. **B493**, 135 (2000); and Phys. Rev. **D63**, 075004 (2001).



- [3] W.D. Goldberger and M. Wise, Phys. Rev. Lett. **83**, 4922 (1999) and Phys. Lett. **475**, 275 (2000); C. Csaki, M. Graesser, L. Randall and J. Terning, Phys. Rev. **D62**, 045015 (2000); C. Charmousis, R. Gregory and V.A. Rubakov, Phys. Rev. **D62**, 067505 (2000); T. Tanaka and X. Montes, Nucl. Phys. **B582**, 259 (2000).
- [4] G.F. Giudice, R. Rattazzi and Wells, Nucl. Phys. **B595**, 250 (2001).
- [5] U. Mahanta and A. Datta, Phys. Lett. **B483**, 196 (2000); T. Han, G.D. Kribs and B. McElrath, Phys. Rev. **D64**, 076003 (2001); M. Chaichian, A. Datta, K. Huitu and Z. Yu, hep-ph/0110035; M. Chaichian, K. Huitu, A. Kobakhidze and Z.-H. Yu, Phys. Lett. **B515**, 65 (2001); S.B. Bae, P. Ko, H.S. Lee and J. Lee, Phys. Lett. **B487**, 299 (2000); S.B. Bae and H.S. Lee, hep-ph/0011275; S.C. Park, H.S. Song and J. Song, hep-ph/0103308; S.R. Choudhury, A.S. Cornell and G.C. Joshi, hep-ph/0012043; K. Cheung, Phys. Rev. **D63**, 056007 (2001).
- [6] G.D. Kribs, in *Proc. of the APS/DPF/DPB Summer Study on the Future of Particle Physics (Snowmass 2001)* ed. R. Davidson and C. Quigg, hep-ph/0110242.
- [7] C. Csaki, M. Graesser, and G.D. Kribs, Phys. Rev. **D63**, 065002 (2001).
- [8] For a recent summary of LEP Higgs boson searches and original references, see A. Sopczak, hep-ph/0112082.
- [9] J. F. Gunion, H. E. Haber, G. L. Kane and S. Dawson, *The Higgs Hunter's Guide*, (Addison-Wesley, Redwood City, CA 1990), SCIPP-89/13.
- [10] M. Battaglia and K. Desch, hep-ph/0101165. See also, M. Carena, D.W. Gerdes, H.E. Haber, A.S. Turcot, and P.M. Zerwas, "Executive Summary of the Snowmass 2001 working group on Electroweak Symmetry Breaking," in *Proc. of the APS/DPF/DPB*

*Summer Study on the Future of Particle Physics*, ed by R. Davidson and C. Quigg, hep-ph/0203229.

[11] D. Dominici, B. Grzadkowski, J. F. Gunion and M. Toharia, arXiv:hep-ph/0206192.

[12] J. L. Hewett and T. G. Rizzo, in *Proc. of the APS/DPF/DPB Summer Study on the Future of Particle Physics (Snowmass 2001)* ed. N. Graf, eConf **C010630**, P338 (2001) [arXiv:hep-ph/0112343]; G. Azuelos *et al.*, “The beyond the standard model working group: Summary report,” proceedings of Workshop on Physics at TeV Colliders, Les Houches, France, 21 May - 1 Jun 2001, arXiv:hep-ph/0204031.

# Shifts in the Properties of the Higgs Boson from Radion Mixing \*

**J.L. Hewett and T.G. Rizzo**

Stanford Linear Accelerator Center  
Stanford University  
Stanford CA 94309, USA

## **Abstract**

We examine how mixing between the Standard Model Higgs boson,  $h$ , and the radion present in the Randall-Sundrum model of localized gravity modifies the expected properties of the Higgs boson. In particular, we demonstrate that the total and partial decay widths of the Higgs, as well as the  $h \rightarrow gg$  branching fraction, can be substantially altered from their Standard Model expectations. The remaining branching fractions are modified less than  $\lesssim 5\%$  for most of the parameter space volume.

---

\*Work supported by the Department of Energy, Contract DE-AC03-76SF00515

The Randall-Sundrum (RS) model of localized gravity [1] offers a potential solution to the hierarchy problem that can be tested at present and future accelerators [2]. In the original version of this model, the Standard Model (SM) fields are confined to one of two branes that are embedded in a 5-dimensional anti-de Sitter space ( $\text{AdS}_5$ ) described by the metric  $ds^2 = e^{-2k|y|}\eta_{\mu\nu}dx^\mu dx^\nu - dy^2$ . The parameter  $k$  characterizes the curvature of the 5-dimensional space and is naturally of order the Planck scale. The two branes form the boundaries of the  $\text{AdS}_5$  slice and gravity is localized on the brane located at  $y = 0$ . Mass parameters on the Standard Model brane, located at  $y = r_c\pi$ , are red-shifted compared to those on the  $y = 0$  brane and are given by  $\Lambda_\pi = \overline{M}_{Pl}e^{-kr_c\pi}$ , where  $\overline{M}_{Pl}$  is the reduced Planck scale. In order to address the hierarchy problem,  $\Lambda_\pi \sim \text{TeV}$  and hence the separation between the two branes,  $r_c$ , must have a value of  $kr_c \sim 11 - 12$ . A number of authors [3] have demonstrated that this quantity can be naturally stabilized by a mechanism which leads directly to the existence of a massive bulk scalar field.

Fluctuations about the stabilized RS configuration allow for two massless excitations described in the metric by  $\eta_{\mu\nu} \rightarrow g_{\mu\nu}(x)$  and  $r_c \rightarrow T(x)$ . The first corresponds to the graviton and  $T(x)$  is a new scalar field arising from the  $g_{55}$  component of the metric and is known as the radion ( $r_0$ ). This scalar field corresponds to a quantum excitation of the brane separation. The mass of the radion is proportional to the backreaction of the bulk scalar vacuum expectation value (vev) on the metric. Generally, one expects that the radion mass should be in the range of a few  $\times 10 \text{ GeV} \leq m_{r_0} \leq \Lambda_\pi$ , where the lower limit arises from radiative corrections and the upper bound is the cutoff of the effective field theory. The radion mass  $m_{r_0}$  is then expected to be below the scale  $\Lambda_\pi$  implying that the radion may be the lightest new field present in the RS model. The radion couples to fields on the Standard Model brane via the trace of the stress-energy tensor with a strength  $\Lambda \propto \Lambda_\pi$  of order the

TeV scale,

$$\mathcal{L}_{eff} = -r_0(x) T_\mu^\mu / \Lambda. \quad (1)$$

Note that  $\Lambda = \sqrt{3}\Lambda_\pi$  in the notation of Ref. [2]. This leads to gauge and matter couplings for the radion that are qualitatively similar to those of the SM Higgs boson. The collider production and decay of the RS radion has been examined by a number of authors [4, 5] and has been recently reviewed by Kribs [6].

On general grounds of covariance, the radion may mix with the SM Higgs field, which is constrained to the TeV brane, through an interaction term of the form

$$S_{rH} = -\xi \int d^4x \sqrt{-g_{ind}} R^{(4)}[g_{ind}] H^\dagger H. \quad (2)$$

Here  $H$  is the Higgs doublet field,  $R^{(4)}[g_{ind}]$  is the Ricci scalar constructed out of the induced metric  $g_{ind}$  on the SM brane, and  $\xi$  is a dimensionless mixing parameter assumed to be of order unity and with unknown sign. The above action induces kinetic mixing between the  $r_0$  and  $h_0$  fields. The resulting Lagrangian can be diagonalized by a set of field redefinitions and rotations [4],

$$\begin{aligned} h_0 &= \cos \rho (h \cos \theta - r \sin \theta), \\ r_0 &= h(\sin \theta - \sin \rho \cos \theta) + r(\cos \theta + \sin \rho \sin \theta), \end{aligned} \quad (3)$$

where  $h, r$  represent the physical fields and

$$\begin{aligned} \tan \rho &= \frac{6\xi v}{\Lambda}, \\ \tan 2\theta &= \frac{2m_{r_0}^2 \sin \rho}{(m_{r_0}^2 - m_{h_0}^2) \cos^2 \rho}, \end{aligned} \quad (4)$$

with  $v \simeq 246$  GeV being the SM vacuum expectation value. The masses of the physical

states are then given by

$$m_{r,h}^2 = \frac{1}{2} \left\{ m_{r_0}^2 (1 + \sin^2 \rho) + m_{h_0}^2 \cos^2 \rho \right. \\ \left. \pm \left[ (m_{h_0}^2 - m_{r_0}^2)^2 \cos^4 \rho + 4m_{r_0}^4 \sin^2 \rho \right]^{1/2} \right\}. \quad (5)$$

This mixing will clearly affect the phenomenology of both the radion and Higgs fields. In particular, the bounds on the Higgs mass from the standard global fit to precision electroweak data are modified, allowing for a Higgs boson (and radion) mass of order several hundred GeV [7]. Here, we examine the modifications to the properties of the Higgs boson, in particular its decay widths and branching fractions, induced by this mixing and find that substantial differences from the SM expectations can be obtained.

To make predictions in this scenario we need to specify four parameters: the masses of the physical Higgs and radion fields, the mixing parameter  $\xi$ , and the ratio  $v/\Lambda$ . Clearly this ratio cannot be too large as  $\Lambda_\pi$  is already bounded from below by collider and electroweak precision data [2]; Tevatron data yields the constraints  $\Lambda_\pi \lesssim 300, 1500, 4500$  GeV for  $k/\overline{M}_{Pl} = 1.0, 0.1, 0.01$ , respectively. Curvature constraints suggest that  $k/\overline{M}_{Pl} \leq 0.1$  [2], which in turn implies  $v/\Lambda \lesssim 0.1$ . For definiteness we will relax this bound somewhat and take  $v/\Lambda \leq 0.2$  along with  $-1 \leq \xi \leq 1$  in our analysis. We note that larger absolute values of  $\xi$  and wider ranges of  $v/\Lambda$  have been entertained in the literature.

The values of the two physical masses themselves are not arbitrary. When we require the mass-squared parameters of the unmixed radion and Higgs fields be real, as is required by hermiticity, we obtain an additional constraint on the ratio of the physical radion and Higgs masses which only depends on the product  $|\xi| \frac{v}{\Lambda}$ . Explicitly one finds that either

$$\frac{m_r^2}{m_h^2} \geq 1 + 2 \sin^2 \rho + 2 |\sin \rho| \sqrt{1 + \sin^2 \rho} \quad (6)$$

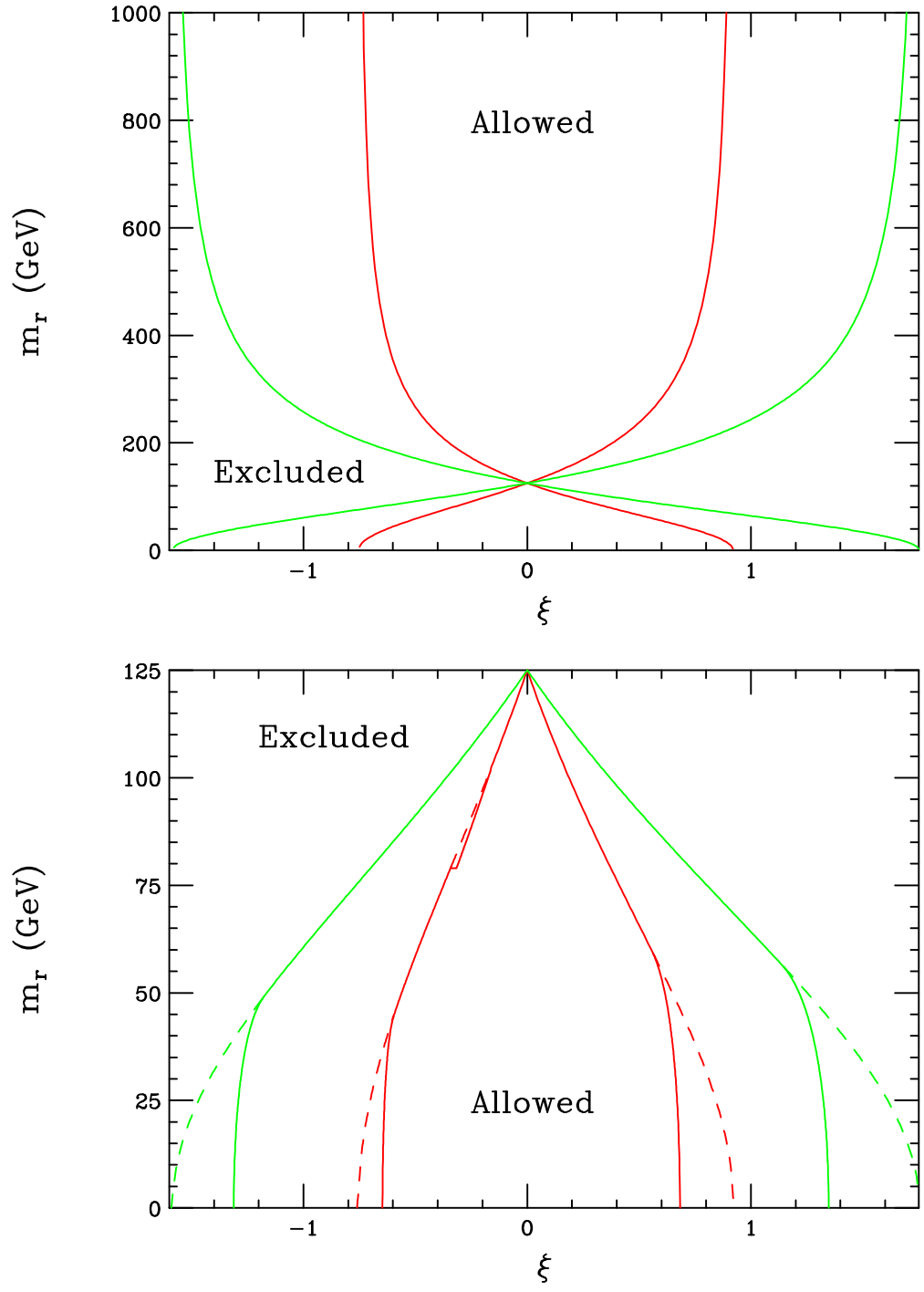


Figure 1: Constraint on the mass of the radion assuming  $m_h = 125$  GeV as a function of the product  $\xi v/\Lambda$  as described in the text. The disallowed region lies between the solid curves. The regions excluded by LEP searches assuming  $v/\Lambda = 0.2$  are also shown and are labeled by ‘LEP’.

or

$$\frac{m_r^2}{m_h^2} \leq 1 + 2 \sin^2 \rho - 2 |\sin \rho| \sqrt{1 + \sin^2 \rho} \quad (7)$$

must hold. Note that it is disfavored for the radion to have a mass near that of the Higgs when there is significant mixing. The resulting excluded region is shown in Fig. 1 for the demonstrative case of  $m_h = 125$  GeV. These constraints are somewhat restrictive; if we take  $\xi \frac{v}{\Lambda} = 0.1$  (0.2) we find that either  $m_r > 205$  (254) GeV or  $m_r < 76$  (61) GeV, assuming  $m_h = 125$  GeV. This low mass region for the radion is partially excluded by direct searches at LEP as also can be seen from the figure. In calculating the LEP constraints, we fixed  $v/\Lambda$  to the conservative value of  $v/\Lambda = 0.2$  while varying  $\xi$ , and converted the LEP Higgs search bounds [8] into constraints for the radion using the appropriate set of rescaling factors. While most of the low mass region for the radion is eliminated for these values of the parameters, the parameter space for a light radion is certainly not closed. As one decreases the assumed fixed value of  $v/\Lambda$ , the size of the allowed low mass region grows since the radion couplings to the  $Z$  are rapidly shrinking. However, one could argue that a somewhat more massive radion is more likely than one in the remaining allowed low mass region.

We now turn our attention to the properties of the Higgs boson in this model when mixing with the radion is included. Following the notation of Giudice *et al.* [4], the couplings of the physical Higgs to the SM fermions and massive gauge bosons  $V = W, Z$  is now given by

$$\mathcal{L} = \frac{-1}{v} (m_f \bar{f} f - m_V^2 V_\mu V^\mu) [\cos \rho \cos \theta + \frac{v}{\Lambda} (\sin \theta - \sin \rho \cos \theta)] h, \quad (8)$$

where the angles  $\rho$  and  $\theta$  are defined above and can be calculated in terms of the four parameters  $\xi$ ,  $v/\Lambda$ , and the physical Higgs and radion masses. Note that the shifts to the fermionic and massive gauge boson couplings are identical. Denoting the combinations  $\alpha = \cos \rho \cos \theta$  and  $\beta = \sin \theta - \sin \rho \cos \theta$ , the corresponding Higgs coupling to gluons can be



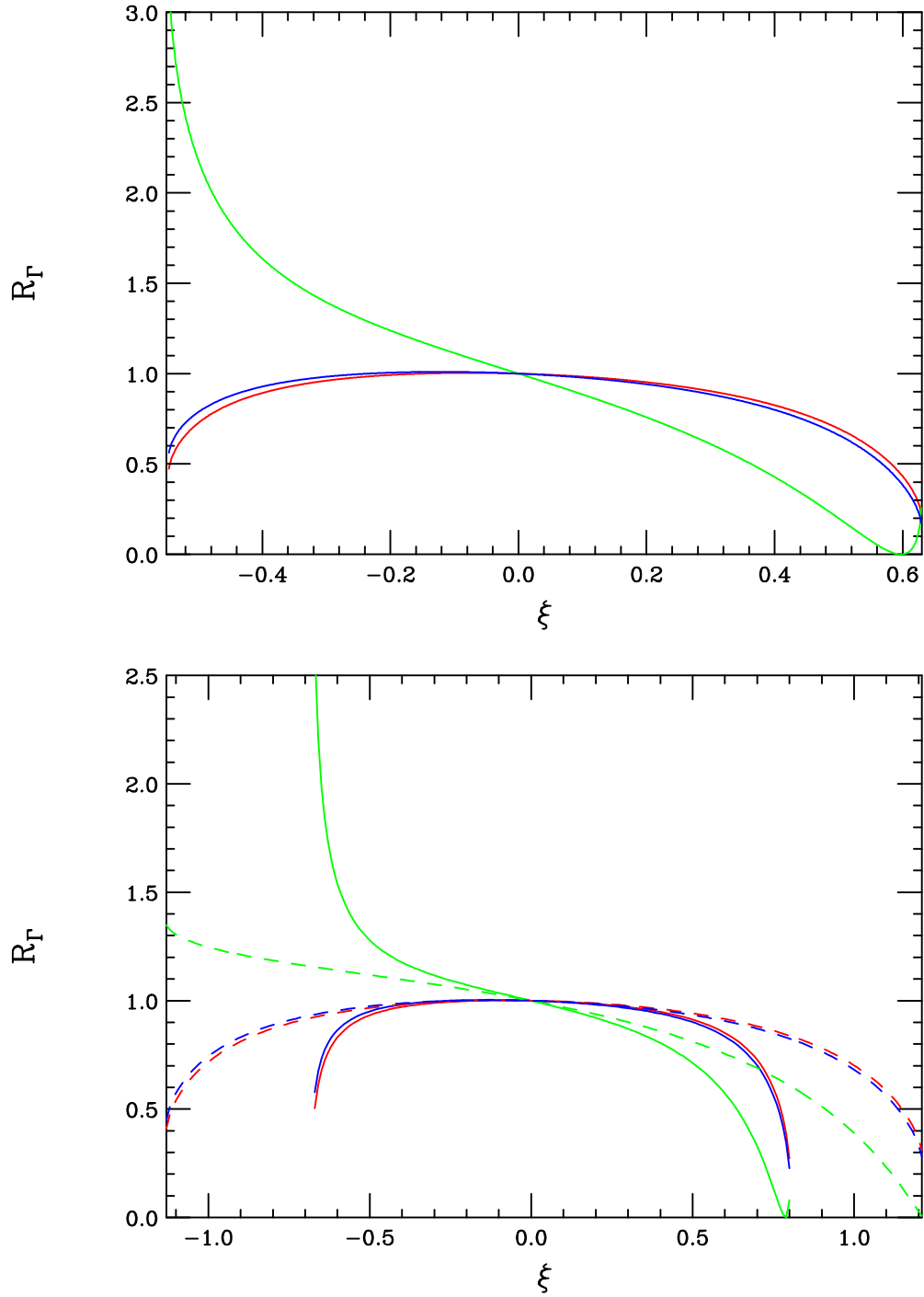


Figure 2: Ratio of Higgs widths to their SM values,  $R_\Gamma$ , as a function of  $\xi$  assuming a physical Higgs mass of 125 GeV: red for fermion pairs or massive gauge boson pairs, green for gluons and blue for photons. This corresponds to gluons, photons,  $V\bar{V}$  from top to bottom on the right. In the top panel we assume  $m_r = 300$  GeV and  $v/\Lambda = 0.2$ . In the bottom panel the solid(dashed) curves are for  $m_r = 500(300)$  GeV and  $v/\Lambda = 0.2(0.1)$ .

written as

$$\mathcal{L} = c_g \frac{\alpha_s}{8\pi} G_{\mu\nu} G^{\mu\nu} h, \quad (9)$$

with

$$c_g = \frac{-1}{2v} \left[ \left( \alpha + \frac{v}{\Lambda} \beta \right) F_g - 2b_3 \beta \frac{v}{\Lambda} \right]. \quad (10)$$

Here, the first term is the usual one-loop top-quark contribution to the  $ggh$  coupling, whereas the second term arises from the trace anomaly and appears solely from the mixing.  $b_3 = 7$  is the  $SU(3)$   $\beta$ -function and  $F_g$  is a well-known kinematic function of the ratio of masses of the top-quark to the physical Higgs boson[9]. Similarly the physical Higgs coupling to two photons is now given by

$$\mathcal{L} = c_\gamma \frac{\alpha_{em}}{8\pi} F_{\mu\nu} F^{\mu\nu} h, \quad (11)$$

where

$$c_\gamma = \frac{1}{v} \left[ - \left( \alpha + \frac{v}{\Lambda} \beta \right) F_\gamma (b_2 + b_Y) \beta \frac{v}{\Lambda} \right]. \quad (12)$$

Here,  $b_2 = 19/6$  and  $b_Y = -41/6$  are the  $SU(2) \times U(1)$   $\beta$ -functions and  $F_\gamma$  is another well-known kinematic function [9] of the ratios of the  $W$  boson and top-quark masses to the physical Higgs mass, and second term again originates from the trace anomaly. Note that in the simultaneous limits  $\alpha \rightarrow 1$ ,  $\beta \rightarrow 0$  we recover the usual SM results. From these expressions we can now compute the modifications to the various decay widths and branching fractions of the SM Higgs due to mixing with the radion.

Fig. 2 shows the ratio of the various Higgs partial widths in comparison to their SM expectations as a function of the parameter  $\xi$  for sample values of  $m_r$  and  $\frac{v}{\Lambda}$  and assuming that  $m_h = 125$  GeV. Several features are immediately apparent: (i) the shifts in the widths to  $\bar{f}f/VV$  and  $\gamma\gamma$  final states are very similar; this is due to the relatively large magnitude of  $F_\gamma$  while the combination  $b_2 + b_Y$  is rather small. (ii) On the otherhand, the shift for the  $gg$

final state can be substantial; here,  $F_g$  is numerically smaller than  $F_\gamma$  and  $b_3$  is quite large, thus yielding a large contribution from the trace anomaly term. (iii) For relatively light radions with a lower value of  $\Lambda$ , the Higgs decay width into the  $gg$  final state can come close to vanishing. This is due to a strong destructive interference between the two contributions to the amplitude for values of  $\xi$  near  $-1$ . (iv) Increasing the value of  $m_r$  has less of an effect than does a decrease in the ratio  $\frac{v}{\Lambda}$ .

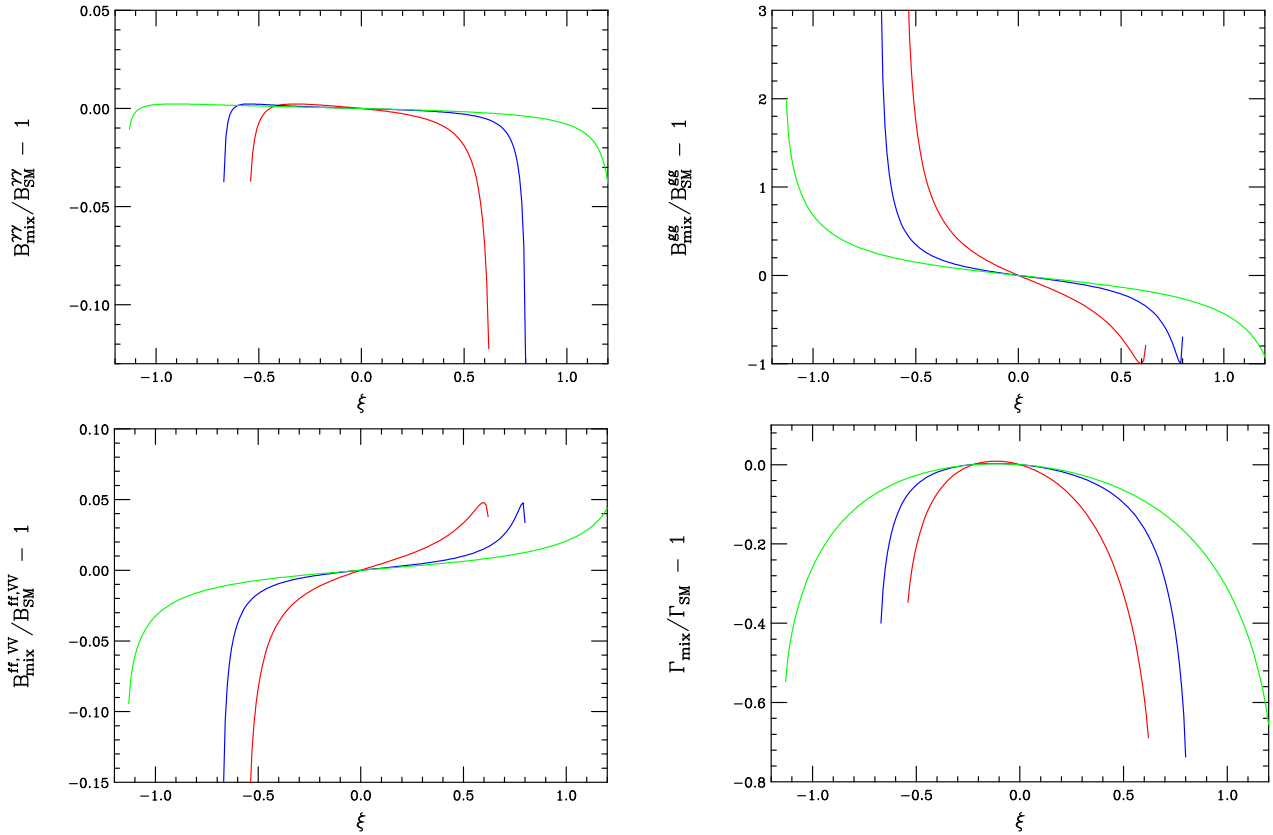


Figure 3: The ratio of the Higgs branching fraction into  $\gamma\gamma$ ,  $gg$ ,  $f\bar{f}$ , and  $VV$  final states as labeled, as well as for the total width, with radion mixing to that of the SM as a function of  $\xi$ . The red (blue; green) curves correspond to the choice  $m_r = 300$  GeV,  $v/\Lambda = 0.2$  (500, 0.2; 300, 0.1).

The deviation from SM expectations for the various branching fractions, as well as the total width, of the Higgs are displayed in Fig. 3 as a function of the mixing parameter  $\xi$ . We see that the gluon branching fraction and the total width may be drastically different than

that of the SM. As we will see below, the former may greatly affect the Higgs production cross section at the LHC. However, the  $\gamma\gamma$ ,  $ff$ , and  $VV$  (where  $V = W, Z$ ) branching fractions only receive small corrections to their SM values, of order  $\lesssim 5 - 10\%$  for almost all of the parameter region. Observation of these shifts will require the precise determination of the Higgs branching fractions which is obtainable at a future high energy  $e^+e^-$  Linear Collider [10]. Once these measurements are performed, constraints on the radion parameter space may be extracted as will be discussed below. These small changes in the  $ZZh$  and  $hb\bar{b}$  couplings of the Higgs boson can also lead to small reductions in the Higgs search reach from LEP. This is presented in Fig. 4 for several sets of parameters; except for extreme cases this reduction in reach is rather modest.

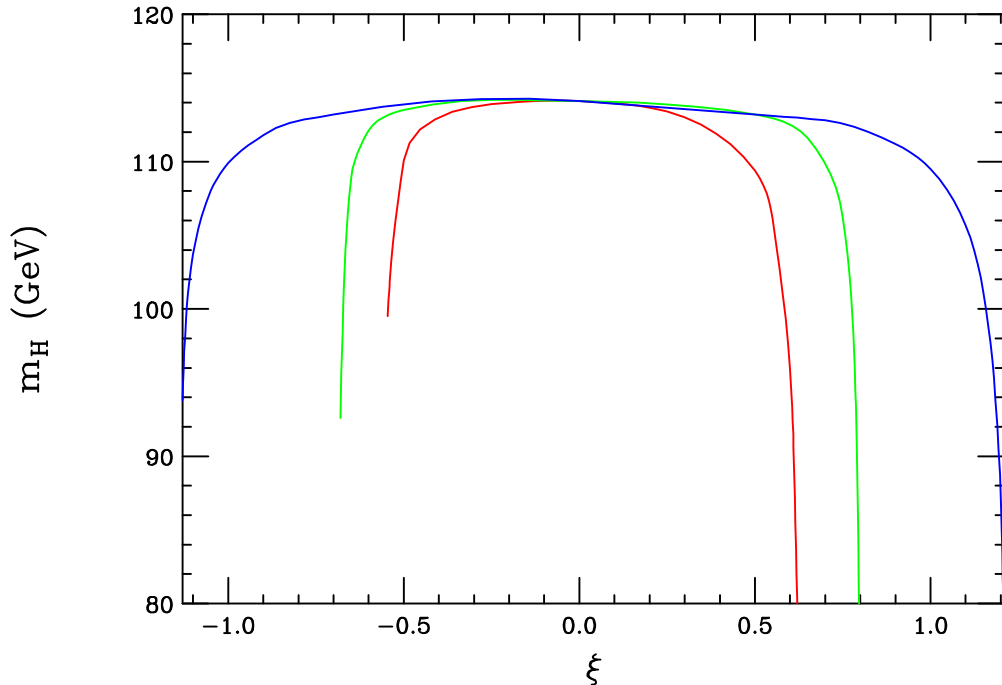


Figure 4: Lower bound on the mass of the Higgs boson from direct searches at LEP as a function of  $\xi$  including the effects of mixing. The red (blue; green) curves correspond to the choice  $m_r = 300$  GeV,  $v/\Lambda = 0.2$  (500, 0.2; 300, 0.1) and represent the curves from bottom to top.

At the LHC, the dominant production mechanism and signal for a light Higgs boson

is gluon-gluon fusion through a triangle graph with subsequent decay into  $\gamma\gamma$ . Both the production cross section and the  $\gamma\gamma$  branching fraction are modified by mixing with the radion, leading to the results illustrated in Fig. 5. This figure shows that the Higgs production rate in this channel at the LHC is always reduced in comparison to the expectations of the SM due to the effects of mixing. For some values of the parameters this reduction can be by more than an order of magnitude which could seriously hinder Higgs discovery via this channel at the LHC.

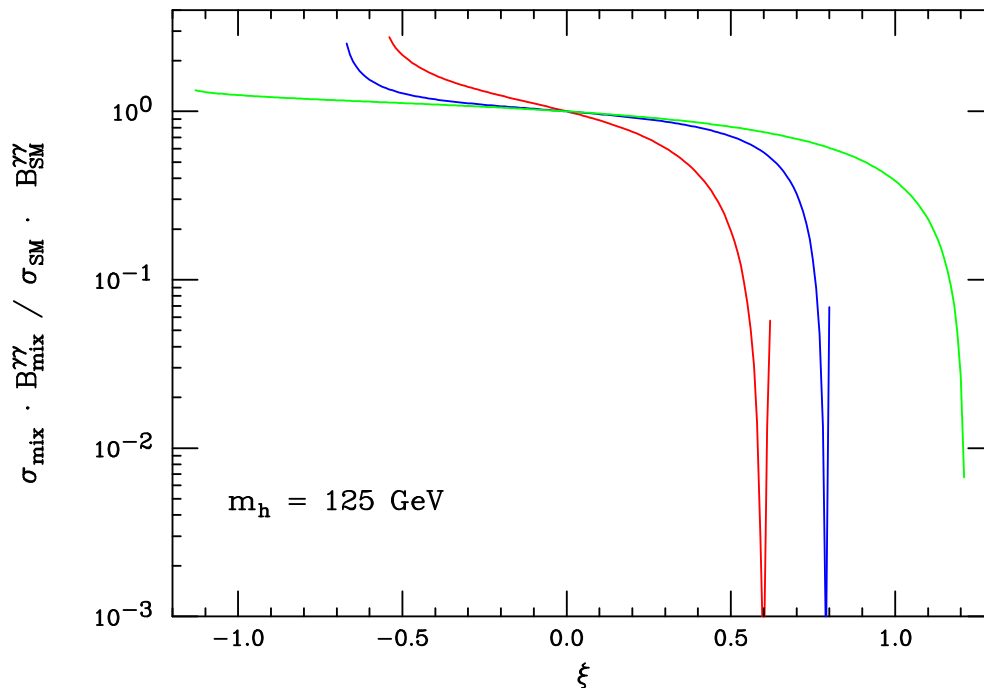


Figure 5: The ratio of production cross section times branching fraction for  $pp \rightarrow h \rightarrow \gamma\gamma$  via gluon fusion with radion mixing to the SM expectations as a function of  $\xi$ . The Higgs mass is taken to be 125 GeV. The red (blue; green) curves correspond to the choice  $m_r = 300$  GeV,  $v/\Lambda = 0.2$  (500, 0.2; 300, 0.1).

The s-channel production of the Higgs boson at a high energy photon photon collider is an important channel for determining the properties of the Higgs. In Fig. 6 we see that decreases in the production rate of the Higgs compared to SM expectations can also occur in the reaction  $\gamma\gamma \rightarrow h \rightarrow b\bar{b}$  when mixing with the radion  $h$  is included. Again, once such mixing is taken into account, the event rate is reduced, possibly hampering the statistical

ability of a future high energy photon collider in measuring the Higgs properties. However, note that the potential reductions in rate for this channel are not as drastic as those which may be realized at the LHC.

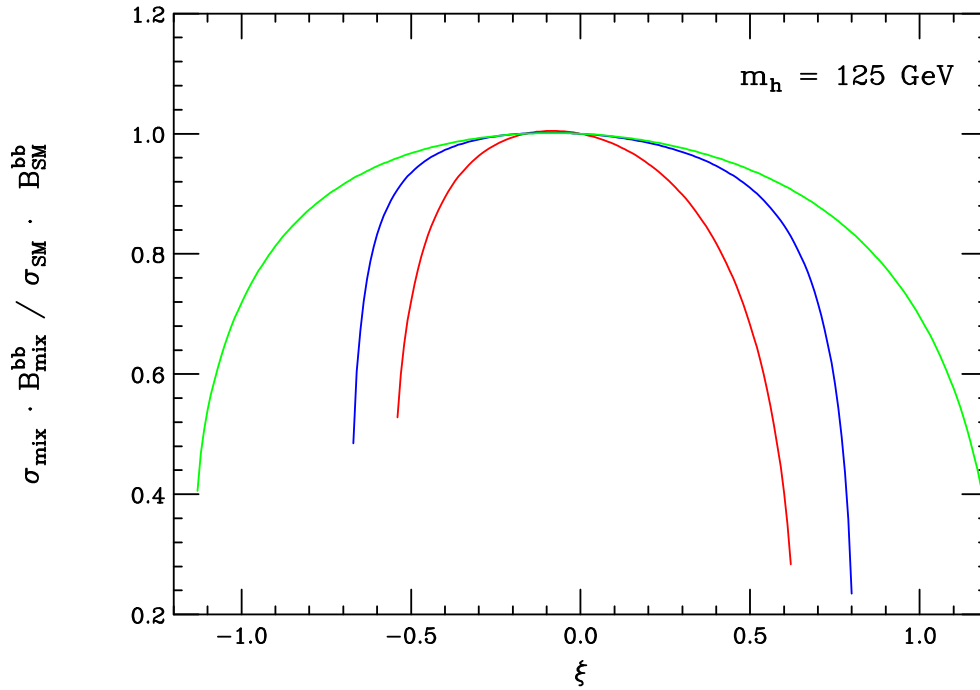


Figure 6: The ratio of production cross section times branching fraction for  $\gamma\gamma \rightarrow h \rightarrow b\bar{b}$  with radion mixing to the SM expectations as a function of  $\xi$ . The Higgs mass is taken to be 125 GeV. The red (blue; green) curves, corresponding to the bottom (middle, top) top curves, represent the parameter choices  $m_r = 300$  GeV,  $v/\Lambda = 0.2$  (500, 0.2; 300, 0.1).

Once data from both the LHC and the Linear Collider (LC) is available, the radion parameter space can be explored using both direct searches and indirect measurements. In fact, the precision measurements of the Higgs boson couplings discussed above can be used to constrain the radion parameter space beyond what may be possible via direct searches for the radion. For purposes of demonstration, let us assume that the LHC and LC determine, within their capabilities, that the Higgs couplings are consistent with the predictions of the SM. Using the expectations for Higgs production at the LHC and LC from the analyses contained in Ref. [10], we derive the resulting excluded regions in the  $\xi - m_r$  parameter

plane. This is displayed in Fig. 7 for various values of  $v/\Lambda$  for the sample case of  $m_h = 125$  GeV. In this figure, the allowed region lies between the corresponding pair of vertical curves. Here, we see that if such a set of measurements of the Higgs properties are realized, then a large fraction of the radion parameter space would be excluded. Direct radion searches at these colliders would fully cover the lower portion of the remaining parameter space up to the radion search reach. Together, the direct and indirect constraints would then only allow for a high mass radion with small mixing as a possibility under this scenario.

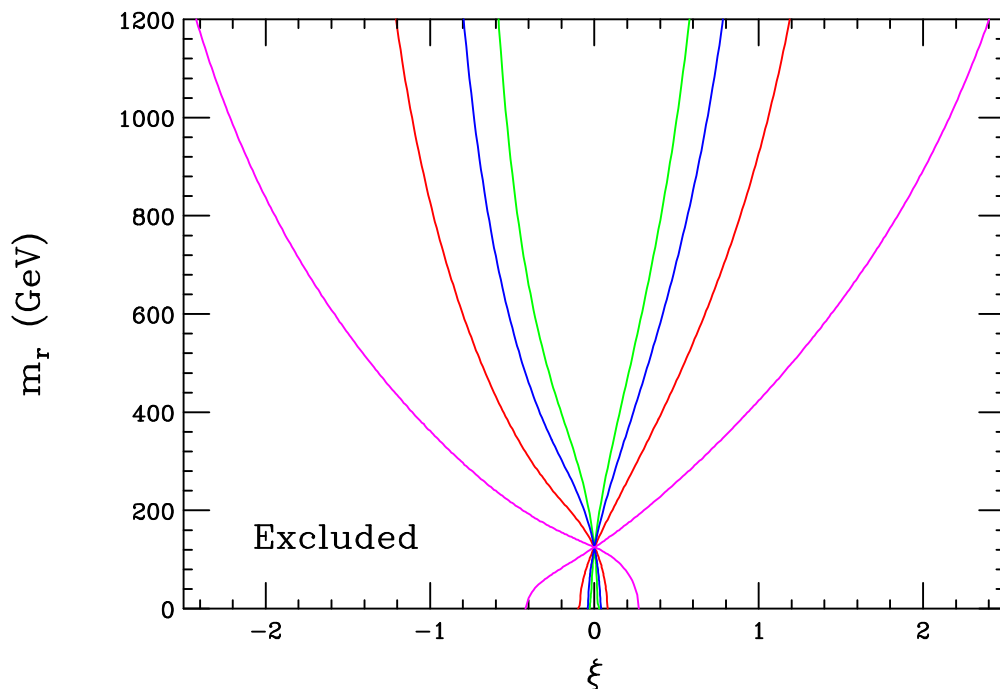


Figure 7: 95% CL indirect bounds on the mass and mixing of the radion arising from the precision measurements of the Higgs couplings obtainable at the LHC and a Linear Collider for a Higgs mass of 125 GeV. The allowed region lies between the corresponding pair of vertical curves. From the inner to outer curves, they represent the parameter values  $v/\Lambda = 0.2, 0.15, 0.10,$  and  $0.05,$  respectively.

Lastly, we note that the patterns of the shifts in the Higgs boson properties due to radion mixing are distinct from those in other models of new physics. For example, consider the two Higgs double model [9]. In this model, the ratio of the  $hVV$  coupling to its SM value is given by  $\sin(\beta - \alpha)$  and the similar ratio for the  $ht\bar{t}$  coupling is  $\cos \alpha / \sin \beta$ , where

$\tan\beta$  is the ratio of vevs of the two Higgs doublets and  $\alpha$  is the mixing angle between the two doublets. In one variant of this model, the corresponding ratio of the  $hb\bar{b}$  coupling is equal, up to a sign, of that for the  $ht\bar{t}$  coupling, while in a second version of the model the  $hb\bar{b}$  ratio is  $-\sin\alpha/\cos\beta$ . In either case, this spectrum of couplings cannot be reproduced via radion mixing.

In summary, we see that Higgs-radion mixing, which is present in some extra dimensional scenarios, can have a substantial effect on the properties of the Higgs boson. These modifications affect the total and partial widths, as well as the branching fractions, of Higgs decay into various final states. This, in turn, can significantly alter the expectations for Higgs production at LEP, the LHC, and a photon collider. For some regions of the parameters, the size of these shifts in the Higgs widths and branching fractions may require the precision of a Linear Collider in order to be studied in detail.

## References

- [1] L. Randall and R. Sundrum, Phys. Rev. Lett. **83**, 3370 (1999); Phys. Rev. Lett. **83**, 4690 (1999).
- [2] For an overview of RS phenomenology, see H. Davoudiasl, J.L. Hewett and T.G. Rizzo, Phys. Rev. Lett. **84**, 2080 (2000); Phys. Lett. **B493**, 135 (2000); and Phys. Rev. **D63**, 075004 (2001).
- [3] W.D. Goldberger and M. Wise, Phys. Rev. Lett. **83**, 4922 (1999) and Phys. Lett. **475**, 275 (2000); C. Csaki, M. Graesser, L. Randall and J. Terning, Phys. Rev. **D62**, 045015 (2000); C. Charmousis, R. Gregory and V.A. Rubakov, Phys. Rev. **D62**, 067505 (2000); T. Tanaka and X. Montes, Nucl. Phys. **B582**, 259 (2000).



- [4] G.F. Giudice, R. Rattazzi and Wells, Nucl. Phys. **B595**, 250 (2001).
- [5] U. Mahanta and A. Datta, Phys. Lett. **B483**, 196 (2000); T. Han, G.D. Kribs and B. McElrath, Phys. Rev. **D64**, 076003 (2001); M. Chaichian, A. Datta, K. Huitu and Z. Yu, hep-ph/0110035; M. Chaichian, K. Huitu, A. Kobakhidze and Z.-H. Yu, Phys. Lett. **B515**, 65 (2001); S.B. Bae, P. Ko, H.S. Lee and J. Lee, Phys. Lett. **B487**, 299 (2000); S.B. Bae and H.S. Lee, hep-ph/0011275; S.C. Park, H.S. Song and J. Song, hep-ph/0103308; S.R. Choudhury, A.S. Cornell and G.C. Joshi, hep-ph/0012043; K. Cheung, Phys. Rev. **D63**, 056007 (2001).
- [6] G.D. Kribs, in *Proc. of the APS/DPF/DPB Summer Study on the Future of Particle Physics (Snowmass 2001)* ed. R. Davidson and C. Quigg, hep-ph/0110242.
- [7] C. Csaki, M. Graesser, and G.D. Kribs, Phys. Rev. **D63**, 065002 (2001).
- [8] For a recent summary of LEP Higgs boson searches and original references, see A. Sopczak, hep-ph/0112082.
- [9] J. F. Gunion, H. E. Haber, G. L. Kane and S. Dawson, *The Higgs Hunter's Guide*, (Addison-Wesley, Redwood City, CA 1990), SCIPP-89/13.
- [10] M. Battaglia and K. Desch, hep-ph/0101165. See also, M. Carena, D.W. Gerdes, H.E. Haber, A.S. Turcot, and P.M. Zerwas, "Executive Summary of the Snowmass 2001 working group on Electroweak Symmetry Breaking," in *Proc. of the APS/DPF/DPB Summer Study on the Future of Particle Physics*, ed by R. Davidson and C. Quigg, hep-ph/0203229.

$$\Gamma_{\text{mix}}^{\text{VV}} / \Gamma_{\text{SM}}^{\text{VV}} - 1$$

